DOI 10.31489/2022No2/58-64

UDC 574.56

PERFORMANCE SIMULATION OF ECO-FRIENDLY SOLAR CELLS BASED ON $CH_3NH_3SnI_3$

Omarova Zh.[1], Yerezhep D.[1]*, Aldiyarov A.[1], Golikov O.[1], Tokmoldin N.[2]

[1*] Faculty of Physics and Technology, Al Farabi Kazakh National University, Almaty Kazakhstan, darhan_13@physics.kz

[2] Optoelectronics of Disordered Semiconductors, Institute of Physics and Astronomy, University of Potsdam, Germany.

Large-scale deployment of the perovskite photovoltaic technology using such high-performance materials as $CH_3NH_3PbI_3$ may face serious environmental issues in the future. Implementation of perovskite solar cell based on Sn could be an alternative solution for commercialisation. This paper presents the results of a theoretical study of a lead-free, environmentally-friendly photovoltaic cell using $CH_3NH_3SnI_3$ as a light-absorbing layer. The characteristics of a photovoltaic cell based on perovskite were modelled using the SCAPS-1D program. Various thicknesses of the absorbing layer were analysed, and an optimised device structure is proposed, demonstrating a high power conversion efficiency of up to 28% at ambient temperature. The analysis of the thicknesses of the $CH_3NH_3SnI_3$ absorbing layer revealed that at a thickness of 500 nm, performance is demonstrated with an efficiency of 27.41 %, a fill factor of 85.92 %, a short circuit current density of 32.60 mA/cm^2 and an open-circuit voltage of 0.98 V. The obtained numerical results indicate that the $CH_3NH_3SnI_3$ absorbing layer may be a viable replacement for the standard materials and may form the basis of a highly efficient technology of the environmentally-friendly perovskite solar cells.

Keywords: lead-free, electron-transport layer, hole-transport layer, absorption layer, SCAPS-1D.

Introduction

With the rapid economic development, the demand for energy is increasing, as evidenced by the studies of the World Energy Resources, which predicted that the world's oil, gas and coal reserves will be exhausted in about 100 years. In addition, a growing number of studies have shown that problems such as environmental pollution and global warming are the consequences of burning fossil fuels [1]. Along with the problem of the depletion of fossil fuels, pollution and global warming pose significant challenges to the production of energy [2,3]. Thus, finding an alternative source that will be clean, renewable and sustainable to replace fossil fuels is an urgent task today. One of the solutions for the production of energy is the conversion of solar energy as photovoltaics is renewable and pure [4]. Besides, it can be converted into many other types of energy for various purposes. Compared with other alternative energy sources, such as hydropower, wind power, bioenergy, geothermal and nuclear power, photovoltaics is available in larger amounts and is more abundant [5].

A photovoltaic cell is an important energy conversion device that uses solar energy [6,7]. The first solar cell was manufactured using a single crystal of silicon at Bell Laboratories, which demonstrated an energy conversion efficiency (PCE) of 6% in 1954 [8]. However, silicon-based photovoltaic cells had their disadvantages, such as high cost and low PCE, but photovoltaic cells based on perovskite prevent all of these disadvantages [9]. Perovskite solar cells (PSC) based on organometallic lead halides quickly emerged as the fourth generation of photovoltaic technology, featuring high PCE [10]. This advantage made them the strongest competitor of silicon-based photovoltaic cells. To date, the PCE of a photovoltaic converter based on perovskites has reached ~ 26 % in a laboratory environment [11–13].

Recently, much attention has been paid to planar perovskite structures (n-i-p or p-i-n) due to the simplicity of the device architecture and, above all, the manufacturability at low temperatures. It allows to facilitate the use of flexible structures as most flexible substrates, such as poly(ethylene 2,6-naphthalate) and poly(ethylene terephthalate), are damaged by the high temperature required for a mesoscopic configuration [14].

Usually, a perovskite photovoltaic material has the following structure: ABX_3, where A is an organic compound CH_3NH_3, B is Pb or Sn, and X_3 is a halide anion (for example, I^-). The most widespread perovskite is $CH_3NH_3PbI_3$, also referred to as MAPI, or a methylammonium lead triiodide. However, perovskites based on MAPI are toxic due to the presence of Pb, which may destabilise the further commercialization of this material [15]. One of the alternative perovskite materials containing tin instead of lead is methylammonium tin triiodide ($CH_3NH_3SnI_3$ or MASI).

A significant amount of research is being dedicated to developing lead-free PSC, with the tin halide perovskite being one of the most promising alternatives [16]. Tin is widely distributed in nature and has similar electronic properties to lead, since it is a member of the same group in the periodic table. In addition, perovskites based on tin halide have excellent light absorbing properties and high carrier mobilities [17]. Additionally, tin-based perovskites provide a high theoretical PCE due to a smaller band gap than the equivalent lead-based perovskites [18].

The transport layer plays a vital role in determining the PCE of a photovoltaic cell. The materials used as the transport layer must fulfil a number of requirements. Firstly, the transport layer must have high transparency for the charge transfer so that the maximum amount of energy enters the perovskite layer. Secondly, it is necessary to have such a material in which the electrons are holes moving fast enough to ensure a rapid charge transfer from one layer to another. It is also necessary to employ a material with good chemical and physical stability in the environment so that it does not react with the other layers of the photovoltaic cell. To collect charge carriers efficiently, it is common to use additional layers such as ETL and HTL. The functional purpose of the ETL is to block holes, collect electrons from the perovskite layer and then deliver them to the anode. Besides, the ETL must have a high transmittance from ultraviolet to the visible regions so that all photons passing through this layer are maximally absorbed by the perovskite. Today, materials used as the ETL include TiO_2, SnO_2, SiO_2, ZnO, etc. In this research, TiO_2 was taken as the ETL since it was possible to achieve the maximum PCE by using this material. Similarly, the functional purpose of the HTL is to block electrons, collect holes from the perovskite layer and then deliver them to the cathode. In this research, Spiro-OMETAD was used as an HTL as this material is widely used as an HTL since the emergence of the first solid perovskite. The key issue for polymer photovoltaic cells based on perovskites is the mobility of the charge carriers. In a photovoltaic cell with a bulk heterojunction, the electron-to-hole mobility ratio can be controlled by replacing one of the donor or acceptor materials.

It should be noted that the experimental research of photovoltaic cell devices is an expensive and laborious process. Therefore, it is common in many scientific fields to perform simulations to obtain an effective structure of a photovoltaic cell. Numerical studies provide opportunities to solve these kinds of problems and help predict/optimize the performance of the device. In this paper, a photovoltaic cell based on perovskites will be modelled using the SCAPS-1D program, which is based on the continuity equations for holes and electrons, as well as the Poisson equation.

Methodology

The simulated photovoltaic cell is shown in Fig. 1 and consists of three main layers: TiO_2 (electron transport layer (ETL))/$CH_3NH_3SnI_3$ (perovskite light-absorbing layer)/Spiro-OMeTAD (hole transport layer (HTL)). It should be noted that recently the numerical analysis in the SCAPS-1D program (version 3.3.09) has become popular as it has proven its effectiveness in various scientific works [19–22]. SCAPS-1D operates by solving the Poisson equation and the continuity equation for electrons and holes. The Poisson equation states:

$$\frac{d^2}{dx^2}\psi(x) = \frac{e}{\varepsilon_0 \varepsilon_r}\left(p(x) - n(x) + N_D - N_A + \rho_p - \rho_n\right), \quad (1)$$

where ψ is the electrostatic potential; e is the elementary charge; ε_0 and ε_r are the dielectric constant in vacuum and the relative dielectric constant of a material; p and n are the concentrations of holes and electrons, respectively; N_D and N_A are the donor and acceptor impurities; ρ_P and ρ_n are the distributions of holes and electrons, respectively.

To describe the dependence of electrons and holes, the following continuity equation is used:

$$\frac{dJ_n}{dx} = G - R, \quad (2)$$

$$\frac{dJ_p}{dx} = G - R, \tag{3}$$

where J_n and J_p are the current density of the electrons and holes; R is the recombination rate; G is the generation rate.

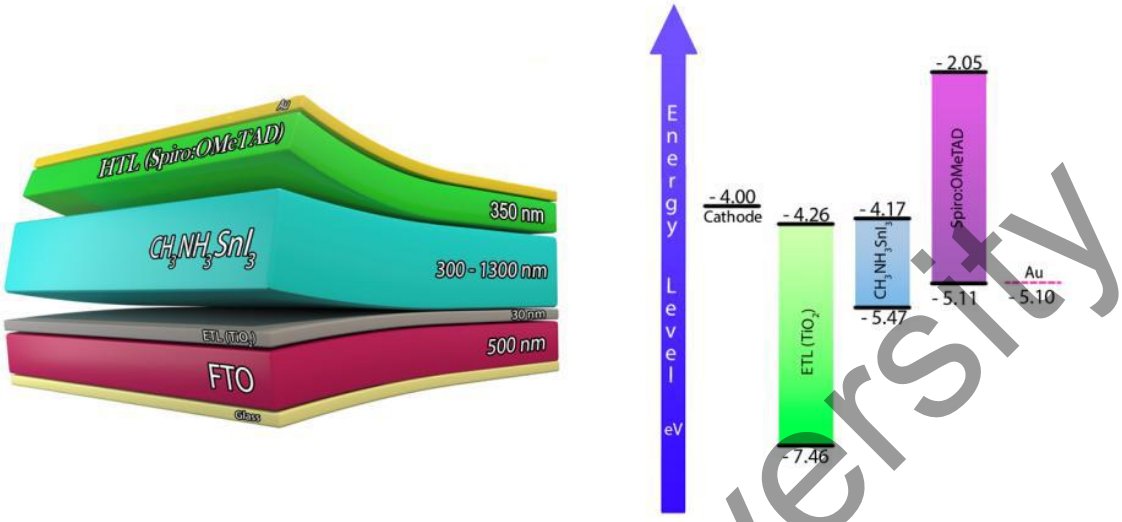

Fig.1. Initial structure of the simulated solar cell

Drift and diffusion move carriers in semiconductors, which can be represented using the equations:

$$J = J_n + J_P, \tag{4}$$

$$J_n = D_n \frac{dn}{dx} + \mu_n n \frac{d\psi}{dx}, \tag{5}$$

$$J_p = D_p \frac{dp}{dx} + \mu_p p \frac{d\psi}{dx}, \tag{6}$$

where J - is the current density; J_n and J_p are the current density of the electrons and holes; D_n and D_p are the diffusion coefficients for electrons and holes; $\frac{dn}{dx}$ and $\frac{dp}{dx}$ are the concentration gradients for electrons and holes; n and p - electron and hole concentrations, μ_n and μ_p - electron and hole mobilities.

The initial technological and geometric parameters of the simulated solar cell were taken from the experimental photovoltaic cell and are presented in Table 1 [19–21]. Table 1 shows the parameters of the semiconductor of each layer as well as the electrical properties of the contacts used in the simulation in this research.

Results and discussion

It should be noted that the optical-electrical characteristics of an organic photovoltaic cell are more dependent on the thickness of the perovskite (absorber) layer. When the thickness of the photovoltaic cell changes, such parameters of the device as short-circuit current, generation and recombination of carriers, mechanism of charge transfer, etc. change as well. Thus, a thicker perovskite layer absorbs more light and generates more electron holes. However, it should be noted that in a thicker layer, the recombination rate increases due to the longer path travelled by the charges, which reduces the PCE of a photovoltaic cell. In this research, the influence of the thickness of the perovskite layer ($CH_3NH_3SnI_3$) on the PCE of a photovoltaic cell was studied through computer simulation. Numerical research was carried out in the AM1.5G solar spectrum at a power of P=1000W/m^2.

Table 1. Parameters of solar cells [19–21].

Parameters	**FTO**	**TiO_2**	**$CH_3NH_3SnI_3$**	**Spiro-OMETAD**
Thickness (nm)	500*	30*	300-1300*	350*
Band gap (eV)	3.50	3.20	1.30	3.06
Electron affinity (eV)	4.00	4.26	4.17	2.05
Dielectric permittivity	9.0	32.0	8.2	3.0
CB effective density of states (cm^{-3})	2.20×10^{18}	1×10^{19}	1×10^{18}	2.20×10^{18}
VB effective density of states (cm^{-3})	1.80×10^{19}	1×10^{19}	1×10^{18}	1.80×10^{19}
Electron thermal speed (cm/s)	1×10^{7}	1×10^{7}	1×10^{7}	1×10^{7}
Hole thermal speed (cm/s)	1×10^{7}	1×10^{7}	1×10^{7}	1×10^{7}
Electron mobility (cm^2/Vs)	20.0	20.0	1.6	2×10^{-4}
Hole mobility (cm^2/Vs)	10.0	10.0	1.6	2×10^{-4}
Shallow donor density N_D (cm-3)	10^{19}	10^{17}	0	0
Shallow acceptor density N_A (cm^{-3})	0	0	1×10^{14}	2×10^{18}
Defect density N_t (cm^{-3})	1.0×10^{14}	1.0×10^{14}	2.5×10^{13}	1.0×10^{15}
*in this research				

Optimisation of the photovoltaic cell was carried out by changing the thickness of the absorbing layer $CH_3NH_3SnI_3$ 300 nm, 500 nm, 700 nm, 900 nm, 1100 nm and 1300 nm at a fixed temperature of 300K, keeping all other parameters and layer thicknesses the same. Considering the complexity of the device and the large choice of materials for PSC, the use of numerical calculation methods allows obtaining important information on the main solar characteristics of the modified PSC. Modelling in SCAPS-1D was done using the parameters shown in Table 1, based on earlier theoretical and experimental works. In this work, the thicknesses of the transport layers were fixed, and special attention was paid to the perovskite absorbing layer. Transport layers play an important role in PSC, because they not only carry cations from the absorbing layer to the electrode, but also act as a separator.

Accordingly, the series resistance of the PSC increases with the increase in the thickness of the charge transport layer, which leads to charge recombination, as it becomes more difficult for holes and electrons to reach the anode and cathode, respectively. Thus, the optimal ETL thickness should be as small as possible to provide good blocking properties at the tops of the layers, resulting in fast electron transfer and low resistive losses [23]. For HTL, the layer thickness is also of great importance, since the minimum time for the charge to pass through the layers will increase the main characteristics of the PSC by increasing the conductivity and reducing the probability of recombination [24–27].

The changes in the thickness of the absorbing layer help determine the best performance of the photovoltaic cell, which can be a decisive factor. Fig. 2 shows the current-voltage characteristics due to different thicknesses of the $CH_3NH_3SnI_3$ absorbing layer.

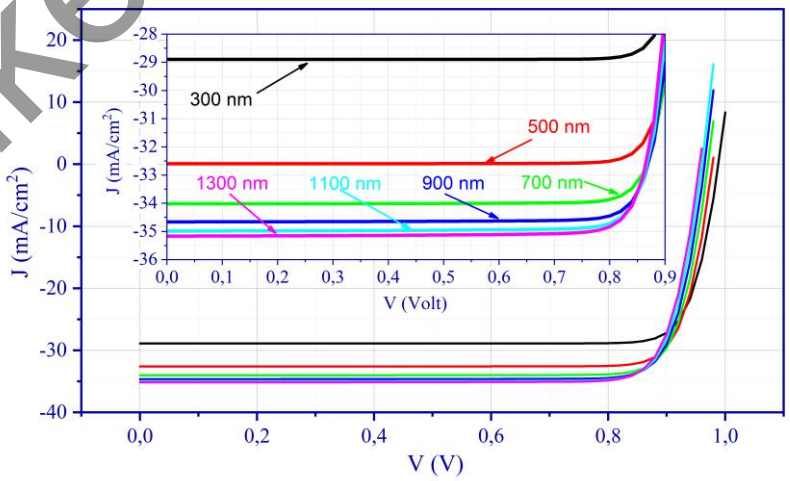

Fig.2. Current-voltage characteristic of a simulated solar cell FTO/TiO_2/$CH_3NH_3SnI_3$/Spiro-OMETAD/Au with different thicknesses of the absorbing layer

It should be noted that the short-circuit current for the absorber layer thickness of 1100-1300 nm is the highest one compared with the other thicknesses. Fig. 3 demonstrates the comparison of the short-circuit current and open-circuit voltage of a tin-based perovskite cell for the thicknesses ranging from 300 nm to 1300 nm.

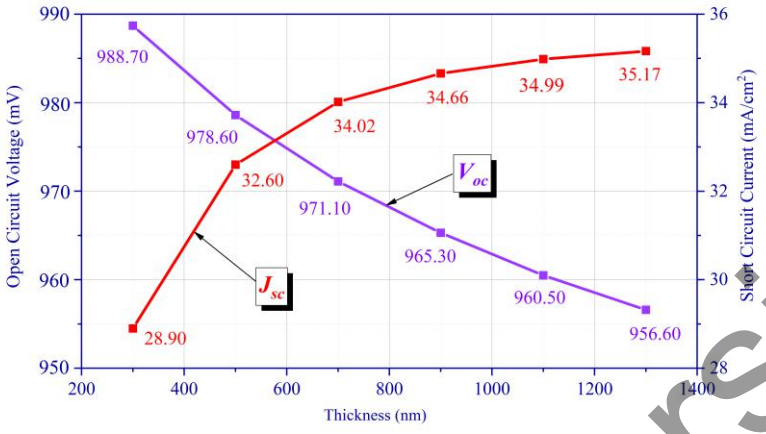

Fig.3. Dependence of the short-circuit current and open-circuit voltage on the thickness

The thickness of the absorber layer plays a significant role in determining the quality and performance of a thin-film PSC. Fig. 4 depicts the changes in the fill factor and PCE with the various thicknesses of the absorbing layer. As can be seen from the figure, the PCE increases with the increase in the thickness of the perovskite layer. However, starting from a thickness of 900 nm, the PCE reaches a plateau and is equal to ~ 29%. It can be seen that as the thickness of the perovskite layer increases, a significant increase in PCE and J_{SC} is observed. This observation can be explained by an increase in the light absorption in the absorbing layer. It facilitates the production of excitons and, therefore, leads to an increase in PCE. However, a further increase in the thickness of the absorber layer to 900 nm leads to higher resistance and higher recombination rates. At first, it leads to a plateau and then to a decrease in the corresponding parameters.

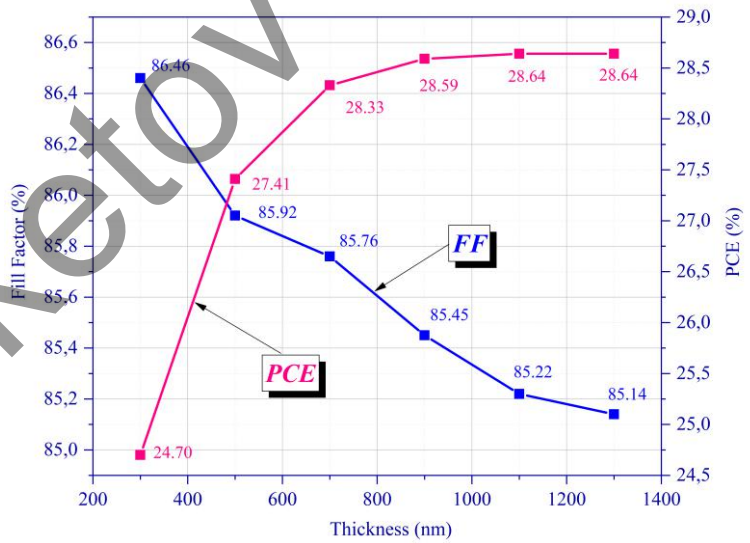

Fig.4. Dependence of the fill factor and PCE on the thickness of the absorbing layer

To prove the reliability of the simulated solar cell, a comparison with the other works on PSCs based on $CH_3NH_3SnI_3$ is shown in Table 2. The analysis of the PCE and the other parameters of the simulated photovoltaic cells the previous studies demonstrated in combination with the results of this research allows to conclude that the model used in this research is reliable. Analyzing works [28–31], one can draw some conclusions regarding the change in the thickness of the absorber layer, in particular, with an increase in the thickness of the absorber, PCE PSC increases, and one can also notice a tendency towards a decrease in FF. This can be explained by the fact that in the case of an increase in the thickness of the absorbing layer, the

energy absorption also increases due to the generation of a larger number of electron-hole pairs. Basically, the decrease in FF is due to the internal recombination of the PSC, which most likely occurs due to the short lifetime of charge carriers (electrons and holes), which leads to a short time for the creation of a conduction band in the PSC.

Table 2. Performance comparison of simulated tin-based PSCs with various device architectures.

Structure	Optimized thickness of the absorber layer (nm)	V_{OC}, V	J_{SC}, mA/cm^2	FF, %	PCE, %	Ref.
TCO//TiO_2/$CH_3NH_3SnI_3$/Spiro-OMETAD/Anode	350	0.67	17.60	44.20	5.15	[28]
FTO/TiO_2/$CH_3NH_3SnI_3$/ Spiro-OMeTAD/Au	350	0.67	16.99	47.67	5.42	[29]
FTO/TiO_2/$CH_3NH_3SnI_3$/ Spiro-OMeTAD/Au	1000	0.91	32.47	65.82	19.51	[30]
FTO/TiO_2/$FASnI_3$/Spiro-OMETAD/Au	2000	1.81	31.20	33.72	19.08	[31]
FTO/TiO_2/$CH_3NH_3SnI_3$/Spiro-OMETAD/Au	1100	0.96	34.99	85.22	28.64	This work

In general, by optimizing the parameters it is possible to achieve a PCE value of ~ 28%, which is an increased PCE value compared to previous works. The simulation results of this work provide the best indicators of the main characteristics of the PCE, which can then be used to predict the efficiency of PSC devices.

Conclusion

In this study, we simulated a lead-free PSC using the structure FTO/TiO_2/$CH_3NH_3SnI_3$/Spiro-OMETAD/Au by means of the SCAPS-1D simulation kit to investigate the performance limit of the given perovskite absorber layer. Particularly, the influence of the active layer thickness on the PCE of the photovoltaic cell was analysed, and the device structure was optimised accordingly. We observe a trade-off between increasing the short-circuit current by enhancing light absorption for the thicker absorber layer and minimizing the loss in the open-circuit voltage and fill factor through carrier recombination for the thinner layer. As a result, this trade-off yields the optimised thickness of the "ideal" perovskite layer free of traps and defects in the range of 1100-1300 nm. This results in the following maximum output cell parameters: J_{SC} = 35.17 mA/cm^2, V_{OC} = 0.96 V, *FF* = 85.14 %, *PCE* = 28.64 %. For comparison, the proposed model of a tin-based PSC with an absorbing layer thickness of 500 nm, which is more standard in terms of fabrication, demonstrates a *PCE* of 27.41 %, a short-circuit current density of 32.60 mA/cm^2, an open-circuit voltage of 0.98 V and a *FF* of 85.92 %. The presented model is intended for further application in the development of environmentally-friendly and lead-free PSCs.

Acknowledgments

These studies have been carried out with the financial support of the Ministry of Education and Science of the Republic of Kazakhstan under grant AP08855738.

The authors acknowledge the provision of SCAPS-1D software by Prof. Marc Burgelman.

REFERENCES

1 Klöckner K., Letmathe P. Is the coherence of coal phase-out and electrolytic hydrogen production the golden path to effective decarbonisation? *Applied Energy*, 2020, Vol. 279, pp. 115779. doi: 10.1016/j.apenergy.2020.115779.

2 Carneiro A.L. et al. Energy consumption and carbon footprint of perovskite solar cells. *Energy Reports*, 2022, Vol. 8, pp. 475–481. doi: 10.1016/j.egyr.2022.01.045.

3 Gür T.M. Carbon Dioxide Emissions, Capture, Storage and Utilization: Review of Materials, Processes and Technologies. *Progress in Energy and Combustion Science*, 2022, Vol. 89, pp. 100965.

4 Martinho F. Challenges for the future of tandem photovoltaics on the path to terawatt levels: a technology review. *Energy & Environmental Science*, 2021, Vol. 14, No. 7, pp. 3840–3871. doi: 10.1039/D1EE00540E.

5 Cousse J. Still in love with solar energy? Installation size, affect, and the social acceptance of renewable

energy technologies. *Renewable and Sustainable Energy Reviews*, 2021, Vol. 145, pp. 111107.

6 Jena A.K., Kulkarni A., Miyasaka T. Halide Perovskite Photovoltaics: Background, Status, and Future Prospects. *Chemical Reviews*, 2019, Vol. 119, No. 5, pp. 3036–3103. doi: 10.1021/acs.chemrev.8b00539.

7 Reddy S.H., Di Giacomo F., Di Carlo A. Low-Temperature-Processed Stable Perovskite Solar Cells and Modules: A Comprehensive Review. *Advanced Energy Materials*, 2022, Vol. 12, No. 13, pp. 2103534.

8 Chapin D.M., Fuller C.S., Pearson G.L. A New Silicon p-n Junction Photocell for Converting Solar Radiation into Electrical Power. *Journal of Applied Physics*, 1954, Vol. 25, No. 5, pp. 676–677. doi: 10.1063/1.1721711.

9 Green M.A. et al. Solar cell efficiency tables (Version 53). *Progress in Photovoltaics: Research and Applications*, 2019, Vol. 27, No. 1, pp. 3–12. doi: 10.1002/pip.3102.

10 Zu F. et al. Illumination-Driven Energy Level Realignment at Buried Interfaces between Organic Charge Transport Layers and a Lead Halide Perovskite. *Solar RRL*, 2022, pp. 2101065. doi: 10.1002/solr.202101065.

11 Jeong M. et al. Stable perovskite solar cells with efficiency exceeding 24.8% and 0.3-V voltage loss. *Science*, 2020, Vol. 369, No. 6511, pp. 1615–1620. doi: 10.1126/science.abb7167.

12 Min H. et al. Perovskite solar cells with atomically coherent interlayers on SnO2 electrodes. *Nature*, 2021, Vol. 598, No. 7881, pp. 444–450. doi: 10.1038/s41586-021-03964-8.

13 Park S.Y., Zhu K. Advances in SnO 2 for Efficient and Stable n–i–p Perovskite Solar Cells. *Advanced Materials*, 2022, pp. 2110438. doi: 10.1002/adma.202110438.

14 Herterich J. et al. Ion Movement Explains Huge V OC Increase despite Almost Unchanged Internal Quasi-Fermi-Level Splitting in Planar Perovskite Solar Cells. *Energy Technology*, 2021, Vol. 9, No. 5, pp. 2001104.

15 Morana M., Malavasi L. Pressure Effects on Lead-Free Metal Halide Perovskites: a Route to Design Optimized Materials for Photovoltaics. *Solar RRL*, 2021, Vol. 5, No. 11, pp. 2100550. doi: 10.1002/solr.202100550.

16 Ghimire S. et al. Structural Reconstruction in Lead-Free Two-Dimensional Tin Iodide Perovskites Leading to High Quantum Yield Emission. *ACS Energy Letters*, 2022, Vol. 7, No. 3, pp. 975–983.

17 Wuttig M. et al. Halide Perovskites: Advanced Photovoltaic Materials Empowered by a Unique Bonding Mechanism. *Advanced Functional Materials*, 2022, Vol. 32, No. 2, pp. 2110166. doi: 10.1002/adfm.202110166.

18 Meier F. et al. Charge Carrier Dynamics of Multiple-Cation Mixed-Halide Perovskite Thin Films. *The Journal of Physical Chemistry C*, 2021, Vol. 125, No. 31, pp. 17411–17417. doi: 10.1021/acs.jpcc.1c04302.

19 Deepthi Jayan K., Sebastian V. Comprehensive device modelling and performance analysis of MASnI3 based perovskite solar cells with diverse ETM, HTM and back metal contacts. *Solar Energy*, 2021, Vol. 217, pp. 40–48.

20 Patel P.K. Device simulation of highly efficient eco-friendly CH3NH3SnI3 perovskite solar cell. *Scientific Reports*, 2021, Vol. 11, No. 1, pp. 3082. doi: 10.1038/s41598-021-82817-w.

21 Singh A.K. et al. Performance optimization of lead free-MASnI3 based solar cell with 27% efficiency by numerical simulation. *Optical Materials*, 2021, Vol. 117, pp. 111193. doi: 10.1016/j.optmat.2021.111193.

22 Kanoun A.-A. et al. Toward development of high-performance perovskite solar cells based on CH3NH3GeI3 using computational approach. *Solar Energy*, 2019, Vol. 182, pp. 237–244. doi: 10.1016/j.solener.2019.02.041.

23 Tariq Jan S., Noman M. Influence of layer thickness, defect density, doping concentration, interface defects, work function, working temperature and reflecting coating on lead-free perovskite solar cell. *Solar Energy*, 2022, Vol. 237, pp. 29–43. doi: 10.1016/j.solener.2022.03.069.

24 Zeinidenov A. et al. The effect of MoO3 interlayer on electro-physical characteristics of the perovskite solar cells. *Synthetic Metals*, 2021, Vol. 281, pp. 116903. doi: 10.1016/j.synthmet.2021.116903.

25 Aimukhanov A.K. et al. Influence of surface structure and morphology of PEDOT: PSS on its optical and electrophysical characteristics. *Bulletin of the Karaganda University. Physics series.*2021, Vol. 103, No. 3, pp. 93–100.

26 Rombach F.M., Haque S.A., Macdonald T.J. Lessons learned from spiro-OMeTAD and PTAA in perovskite solar cells. *Energy & Environmental Science*, 2021, Vol. 14, No. 10, pp. 5161–5190. doi: 10.1039/D1EE02095A.

27 Aimukhanov A.K. et al. The influence of structural and charge transport properties of <scp>PEDOT</scp> : <scp>PSS</scp> layers on the photovoltaic properties of polymer solar cells. *Polymers for Advanced Technologies*, 2021, Vol. 32, No. 2, pp. 497–504. doi: 10.1002/pat.5102.

28 Salem M.S. et al. Analysis of Hybrid Hetero-Homo Junction Lead-Free Perovskite Solar Cells by SCAPS Simulator. *Energies*, 2021, Vol. 14, No. 18, pp. 5741. doi: 10.3390/en14185741.

29 Abdelaziz S. et al. Investigation of lead-free MASnI3-MASnIBr2 tandem solar cell: Numerical simulation. *Optical Materials*, 2022, Vol. 123, pp. 111893. doi: 10.1016/j.optmat.2021.111893.

30 Deepthi Jayan K., Sebastian V. Comprehensive device modelling and performance analysis of MASnI3 based perovskite solar cells with diverse ETM, HTM and back metal contacts. *Solar Energy*, 2021, Vol. 217, pp. 40–48.

31 Kumar M. et al. An optimized lead-free formamidinium Sn-based perovskite solar cell design for high power conversion efficiency by SCAPS simulation. *Optical Materials*, 2020, Vol. 108, pp. 110213.

Article accepted for publication 25.03.2022